Abundance of CuZn+SnZn and 2CuZn+SnZn defect clusters in kesterite solar cells

Shiyou Chen, Lin-Wang Wang, Aron Walsh, X. G. Gong, and Su-Huai Wei

Related Articles

Exploiting piezoelectric charge for high performance graded InGaN nanowire solar cells
Appl. Phys. Lett. 101, 143905 (2012)

Design principles for plasmonic thin film GaAs solar cells with high absorption enhancement
J. Appl. Phys. 112, 054326 (2012)

Optical absorptions in AlxGa1−xAs/GaAs quantum well for solar energy application
J. Appl. Phys. 112, 054314 (2012)

Analyzing nanotextured transparent conductive oxides for efficient light trapping in silicon thin film solar cells
Appl. Phys. Lett. 101, 103903 (2012)

Subbandgap current collection through the implementation of a doping superlattice solar cell
Appl. Phys. Lett. 101, 073901 (2012)

Additional information on Appl. Phys. Lett.

Journal Homepage: http://apl.aip.org/

Journal Information: http://apl.aip.org/about/about_the_journal

Top downloads: http://apl.aip.org/features/most_downloaded
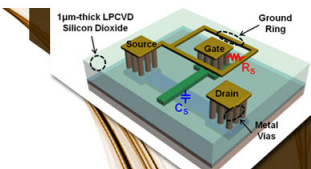
Information for Authors: http://apl.aip.org/authors

Abundance of $Cu_{Zn} + Sn_{Zn}$ and $2Cu_{Zn} + Sn_{Zn}$ defect clusters in kesterite solar cells

Shiyou Chen,[1,2] Lin-Wang Wang,[2] Aron Walsh,[3] X. G. Gong,[4] and Su-Huai Wei[5]

[1]*Key Laboratory of Polar Materials and Devices (MOE), East China Normal University, Shanghai 200241, China*
[2]*Joint Center for Artificial Photosynthesis (JCAP), Lawrence Berkeley National Laboratory, Berkeley, California 94720, USA*
[3]*Key Laboratory for Computational Physical Sciences (MOE) and Surface Physics Laboratory, Fudan University, Shanghai 200433, China*
[4]*Center for Sustainable Chemical Technologies and Department of Chemistry, University of Bath, Claverton Down, Bath BA2 7AY, United Kingdom*
[5]*National Renewable Energy Laboratory, Golden, Colorado 80401, USA*

Kesterite solar cells show the highest efficiency when the absorber layers (Cu_2ZnSnS_4 [CZTS], $Cu_2ZnSnSe_4$ [CZTSe] and their alloys) are non-stoichiometric with $Cu/(Zn + Sn) \approx 0.8$ and $Zn/Sn \approx 1.2$. The fundamental cause is so far not understood. Using a first-principles theory, we show that passivated defect clusters such as $Cu_{Zn} + Sn_{Zn}$ and $2Cu_{Zn} + Sn_{Zn}$ have high concentrations even in stoichiometric samples with $Cu/(Zn+Sn)$ and Zn/Sn ratios near 1. The partially passivated $Cu_{Zn} + Sn_{Zn}$ cluster produces a deep donor level in the band gap of CZTS, and the fully passivated $2Cu_{Zn} + Sn_{Zn}$ cluster causes a significant band gap decrease. Both effects are detrimental to photovoltaic performance, so Zn-rich and Cu, Sn-poor conditions are required to prevent their formation and increase the efficiency. The donor level is relatively shallower in CZTSe than in CZTS, which gives an explanation to the higher efficiency obtained in $Cu_2ZnSn(S, Se)_4$ (CZTSSe) cells with high Se content. © *2012 American Institute of Physics*. [http://dx.doi.org/10.1063/1.4768215]

The development of thin film solar cells using the earth-abundant kesterite Cu_2ZnSnS_4 (CZTS) and $Cu_2ZnSnSe_4$ (CZTSe) semiconductors as the light-absorber layer has rapidly progressed over the past three years,[1–3] e.g., a 10.1% efficiency has been achieved by Barkhouse *et al.* in CZTSSe cells,[4,5] and 9.2% by Repins *et al.* in CZTSe cells.[6] Despite the ideal electronic properties for visible light absorption (band gaps around 1.0 and 1.5 eV, respectively, and high optical absorption coefficients[7–9]), the increased number of elements makes it challenging to synthesize high-quality single-crystal samples, i.e., non-stoichiometry and the coexistence of secondary compounds are frequently observed.[10–14] One unusual observation is that all the kesterite solar cells with reported efficiencies higher than 8% have the element ratios $Cu/(Zn + Sn) \approx 0.8$ and $Zn/Sn \approx 1.2$,[1,4,6,15,16] seriously deviating from the ideal value of 1. This has resulted in an empirical rule that the Cu poor and Zn rich growth condition gives the highest efficiency.[3,14,15,17,18] Typically, such high level of non-stoichiometry indicates either the high population of intrinsic defects or the coexistence of secondary compounds (e.g., low $Cu/(Zn+Sn)$ and high Zn/Sn ratios may be caused by ZnS coexistence), which can have detrimental influence and cause the photovoltaic performance worse than that of the stoichiometric cell. Why do then kesterites exhibit the opposite effect?

One possible explanation is that when $Cu/(Zn + Sn) \approx 1$ and $Zn/Sn \approx 1$, intrinsic defects that act as recombination centers (deep donors or acceptors) are formed, which can be eliminated when the environment becomes Zn-rich and Cu, Sn-poor. In the chalcopyrites $CuGaSe_2$ (CGSe) and $CuInSe_2$ (CISe), Ga_{Cu} and In_{Cu} antisite defects have been reported as deep donors, and are considered as the limiting factors of the

$Cu(In, Ga)Se_2$ based solar cell efficiency.[19,20] Similarly, we may ask if such kind of antisite defects also produce deep donor levels in CZTS and CZTSe. Previously, Sn_{Cu} and Sn_{Zn} donor levels are found to be deep,[21–23] but their formation energies are high, even when they are fully ionized in p-type samples,[21,22] so their population is rather low and their influence is weak.

In this letter, we show using the first-principles calculations that the compensation between the dominant acceptor defect Cu_{Zn} and the donor defect Sn_{Zn} can decrease the formation energies of the defect clusters ($Cu_{Zn} + Sn_{Zn}$ and $2Cu_{Zn} + Sn_{Zn}$) significantly, so they have high concentration in stoichiometric samples with $Cu/(Zn + Sn) \approx 1$ and $Zn/Sn \approx 1$. In CZTS, the partially compensated $Cu_{Zn} + Sn_{Zn}$ cluster produces deep donor levels and the fully compensated $2Cu_{Zn} + Sn_{Zn}$ induces a significant band gap decrease. Both effects can contribute to the low efficiency of stoichiometric CZTS and CZTSe solar cells. These states are relatively shallow in CZTSe compared to CZTS, which explains the higher efficiency of the CZTSSe solar cells when the Se composition is higher.[1,3,15]

In kesterite CZTS (CZTSe), each anion is tetrahedrally coordinated by four cations (two Cu in the nominal valence +1, one Zn in +2, and one Sn in +4). When Cu replaces Zn (Cu_{Zn} antisite), an acceptor level is produced above the valence band maximum (VBM), and when Sn replaces Zn (Sn_{Zn} antisite), two electrons occupy a donor level below the conduction band minimum (CBM), as shown in Fig. 1. Aggregation of these defects results in electronic compensation and Coulombic attraction: electron transfer from the donor to acceptor state (see Fig. 1) decreases the formation energy of the $Cu_{Zn} + Sn_{Zn}$ cluster. Since Sn_{Zn} is a double
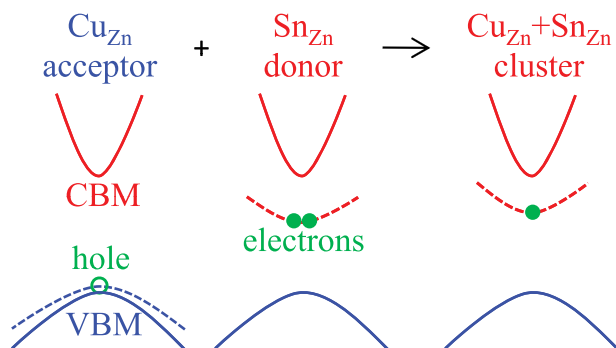
FIG. 1. An illustration of the compensation between the Cu_{Zn} with an empty acceptor level and Sn_{Zn} with a donor level occupied by two electrons. When Cu_{Zn} binds with Sn_{Zn}, the compensation leads to the formation of the defect cluster $Cu_{Zn} + Sn_{Zn}$, which has a partially occupied deep donor level at neutral charge state.

donor defect, $Cu_{Zn} + Sn_{Zn}$ still has one donor electron that can compensate another Cu_{Zn} acceptor, forming the $2Cu_{Zn} + Sn_{Zn}$ tri-cluster. Due to the strength of the attractive interactions, these compensated defect clusters can have high populations in the synthesized samples. This is similar to the case that high-population $2V_{Cu} + In_{Cu}$ and $2V_{Cu} + Ga_{Cu}$ clusters have been observed in the chalcopyrites.[24,25] In our study, the populations of $Cu_{Zn} + Sn_{Zn}$ and $2Cu_{Zn} + Sn_{Zn}$ clusters in CZTS and CZTSe can be predicted through calculation of the defect formation energies and statistical models.

The defect formation energy is calculated following the standard approach,[26,27] i.e., a defect α with a charge state q is created in a 128-atom supercell. The resulting formation energy is explicitly dependent on the chemical environment (elemental chemical potentials μ_i, where $i = Cu, Zn, Sn, S$) and the Fermi energy (electron chemical potential, E_F). The total energy calculations were performed using the VASP code,[28] with the PW91 exchange correlation functional, a plane wave cutoff energy of 300 eV, and a $2 \times 2 \times 1$ k-point mesh. Band gap corrections ($\Delta_{VBM} = 0.40$ and 0.39 eV for CZTS and CZTSe, respectively) were determined using the procedure as given for CGSe and CISe in Ref. 29, and further technical details can be found in Ref. 22.

In Fig. 2, the formation energies of several low-energy defects and defect clusters in (a) CZTS and (b) CZTSe are plotted as a function of the elemental chemical potentials shown in (c). Because the Cu_{Zn} antisite is the dominant acceptor defect in both CZTS and CZTSe under these conditions,[21,22,30] the samples are inherently p-type, so E_F will be close to the VBM (equal to 0 eV), which makes the donor defects such as Sn_{Zn}^{2+}, $[Cu_{Zn} + Sn_{Zn}]^{+}$, and Zn_{Cu}^{+} ionized with a lower formation energy than in the neutral state. The element chemical potentials (μ_{Cu}, μ_{Zn}, and μ_{Sn}) describe the richness of the elements, and are limited to a certain range to avoid the formation of the competitive compounds, which has been discussed in detail previously for CZTS.[21,22] In Fig. 2(c), the chemical potential range that stabilizes CZTSe is shown by the black region surrounded by the points P-Q-M-N. Due to the competitive secondary phases ZnSe and Cu_2SnSe_3, μ_{Zn} is limited to a very narrow range, i.e., too much Zn (higher μ_{Zn}) leads to ZnSe formation while too little Zn (lower μ_{Zn}) leads to Cu_2SnSe_3 formation.
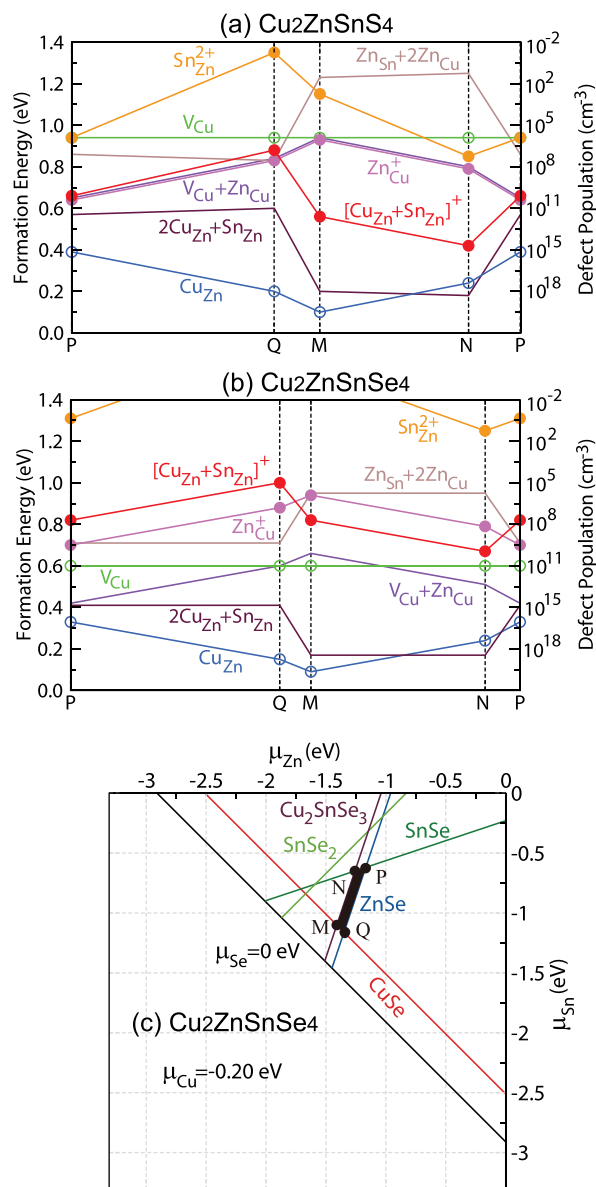

FIG. 2. The calculated formation energies of low-energy defects and defect clusters in p-type CZTS (a) and CZTSe (b) under their stable chemical potential conditions. The Fermi energy is set at the VBM, so all the donor defects are fully ionized. The chemical potential points P-Q-M-N of CZTSe are given in (c) and those of CZTS can be found in Ref. 21.

Population of defect clusters in CZTS. It is clear in Fig. 2(a) that the $Cu_{Zn} + Sn_{Zn}$ and $2Cu_{Zn} + Sn_{Zn}$ have low formation energies in the stable chemical potential range, corresponding to a population of the order of $10^7 - 10^{15}$ and $10^{10} - 10^{18}$ cm^{-3} in CZTS, respectively. When the chemical potentials are near the M-N line, their population can be as high as 10^{15} and 10^{18} cm^{-3}, respectively, which is easy to understand since Cu_2SnS_3 is stabilized if μ_{Zn} is on the left side of the M-N line (Zn poor) and the formation of $2Cu_{Zn} + Sn_{Zn}$ can convert CZTS towards Cu_2SnS_3. In the stable chemical potential region, all defects (including the dominant Cu_{Zn}) have populations lower than 10^{20} cm^{-3}, which corresponds to deviation in Cu/(Zn+Sn) and Zn/Sn ratios by less than 0.01. CZTS samples under these conditions have Cu/(Zn+Sn) and Zn/Sn ratios around one, which indicates that even in stoichiometric samples a high population of $Cu_{Zn} + Sn_{Zn}$ and $2Cu_{Zn} + Sn_{Zn}$ defect clusters can still exist.

On the other hand, defect formation with populations lower than 10^{20} cm^{-3} cannot cause a large deviation of the element ratios as in the high-efficiency solar cells (Cu/(Zn + Sn) ≈ 0.8 and Zn/Sn ≈ 1.2). These materials must be synthesized under conditions beyond the stable chemical potential region of CZTS, e.g., on the right hand side of P-Q line. When μ_{Zn} is higher than P-Q line (Zn rich), the high population of defects such as $V_{Cu} + Zn_{Cu}$ and $Zn_{Sn} + 2Zn_{Cu}$ as well as the coexistence of ZnS can cause Cu/(Zn + Sn) ≈ 0.8 and Zn/Sn ≈ 1.2, but the population of $Cu_{Zn} + Sn_{Zn}$ and $2Cu_{Zn} + Sn_{Zn}$ can be decreased dramatically, so their detrimental influence on photovoltaic performance can be reduced.

Electronic state of defect clusters. The charge density of the $Cu_{Zn} + Sn_{Zn}$ donor state is shown in Fig. 3, which is localized around the Sn_{Zn} antisite with almost no distribution around Cu_{Zn}. The combination of Sn 5*s* and S 3*p* orbitals is the characteristic of Sn_{Zn} related donor defects. When Sn replaces Zn in the CZTS lattice, two Sn 5*p* electrons are transferred to S, while the 5*s* orbital forms a localized donor state. The Sn 5*s* orbital is much lower in energy than the 5*p* orbital (see Table II of Ref. 31), which is also why Sn is stable in two oxidation states.[23,32] Using a hybrid density functional (HSE06), which performs well for CZTS,[33–35] we predict the localized donor state (eigenvalue) to be 1.03 eV below the CBM (for one Sn_{Zn} antisite in the 128-atom CZTS supercell).

Binding of Sn_{Zn} and Cu_{Zn} leads to level repulsion between the donor and acceptor states, thus pushes the energy of the donor state to 0.63 eV below the CBM, which can be seen in the calculated density of states (DOS) plotted in Fig. 4 (top panel). A small peak ($\sim$0.6 eV below the CBM) is located in the middle of the CZTS band gap, which is mainly composed of Sn 5*s* states (as shown by the projected DOS). To describe the ionization of this donor defect more accurately, we have also calculated the optical and thermal transition energy levels,[19,26] and found the values
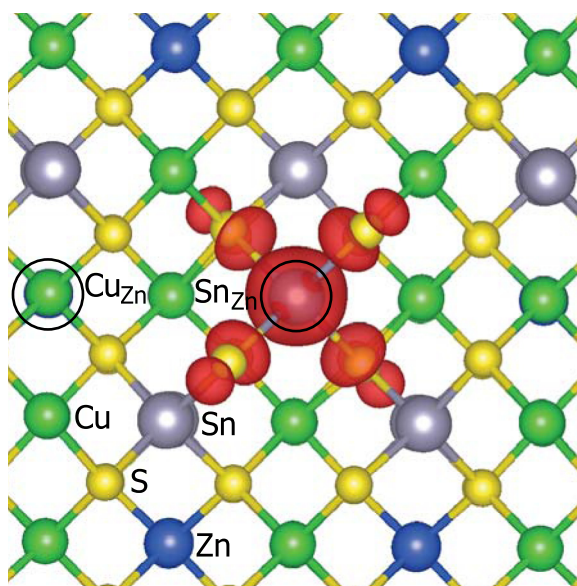

FIG. 3. Electron density isosurface of the $Cu_{Zn} + Sn_{Zn}$ donor state (isovalue 25% of the maximum value). The green, blue, gray, and yellow filled circles show Cu, Zn, Sn, and S atoms, respectively, and the black circles show the defect sites of Cu_{Zn} and Sn_{Zn}.
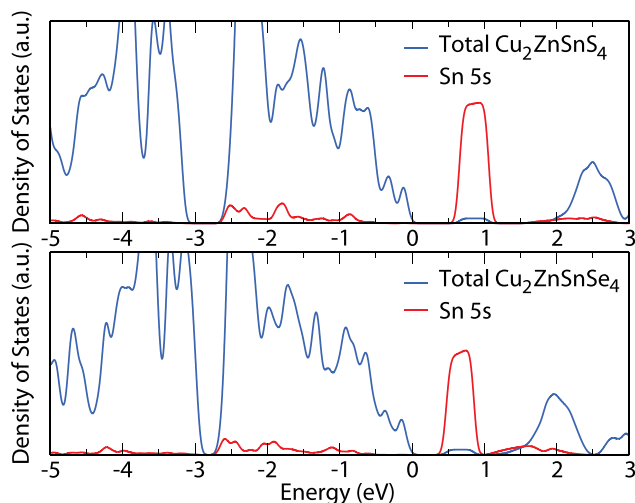

FIG. 4. Calculated DOS of CZTS (top) and CZTSe (bottom) with a $Cu_{Zn} + Sn_{Zn}$ defect cluster in a 128-atom supercell. The blue lines show the total DOS and the red lines show the projected DOS on Sn 5*s* orbital at the Sn_{Zn} site (multiplied by 128 for clarity). The energy is relative to the VBM of CZTS and CZTSe.

for the (0/+) transition are 0.85 and 0.33 eV below the CBM, respectively. In contrast, the $2Cu_{Zn} + Sn_{Zn}$ complex is fully compensated, so there is no occupied donor state. The change in potential does, however, cause a CBM red-shift by 0.2 eV (a total band gap decrease by 0.35 eV due to an additional VBM upshift of 0.15 eV). It should be noted that for Sn_{Zn}, $Cu_{Zn} + Sn_{Zn}$, and $2Cu_{Zn} + Sn_{Zn}$, the localization of the Sn 5*s* state on the defect site is always kept (see Fig. 3), which indicates that a high population of these defects will either produce deep recombination centers for electron-hole pairs, or cause strong electron trapping, both detrimental to the photovoltaic efficiency. Considering the high population of both defect clusters even in the stoichiometric CZTS samples, we can understand the limited efficiency of stoichiometric kesterite solar cells. In contrast, when Cu/(Zn + Sn) ≈ 0.8 and Zn/Sn ≈ 1.2, high μ_{Zn}, low μ_{Cu} and μ_{Sn} conditions are required, so the populations of both defect clusters are decreased and a higher efficiency is expected.

Defect clusters in CZTSe. Since solar cells based on the CZTSSe alloy are found to show higher efficiency when the Se composition is high,[1,3,15] now we will try to reveal if this is also related to $Cu_{Zn} + Sn_{Zn}$ and $2Cu_{Zn} + Sn_{Zn}$. In Fig. 2(b), the calculated formation energies in CZTSe are plotted. Comparing the values in CZTSe and in CZTS, it can be found that: (i) the population of $Cu_{Zn} + Sn_{Zn}$, which produces deep donor levels, is between 10^5 and 10^9 cm^{-3} in CZTSe, lower than the corresponding value in CZTS; (ii) the population of $2Cu_{Zn} + Sn_{Zn}$ is always high, between 10^{15} and 10^{19} cm^{-3}, even higher than that in CZTS. However, the Sn_{Zn} induced donor levels (eigenvalues) are 0.35, 0.23, and 0.12 eV below the CBM for isolated Sn_{Zn}, $Cu_{Zn} + Sn_{Zn}$ (see the calculated DOS in Fig. 4, bottom panel), and $2Cu_{Zn} + Sn_{Zn}$ clusters, respectively, consistently shallower than in CZTS (1.03, 0.63, 0.20 eV, respectively). Thus, high population of $2Cu_{Zn} + Sn_{Zn}$ in CZTSe is not too harmful. The results above show that the effects of both $Cu_{Zn} + Sn_{Zn}$ and $2Cu_{Zn} + Sn_{Zn}$ clusters are therefore weaker in CZTSe. This gives an explanation to the higher efficiency observed when

Se composition is high. It also suggests that the more negative influence of these defect clusters in CZTS imposes a limit to the efficiency of CZTSSe alloys, i.e., although increasing the S composition can increase the band gap of the absorber layer closer to the optimal value (1.4–1.5 eV according to the Shockley-Queisser model), the efficiency may be decreased when S composition is high due to the formation of the deep trap states that limit carrier life time.

In conclusion, we reveal that $Cu_{Zn} + Sn_{Zn}$ and $2Cu_{Zn} + Sn_{Zn}$ clusters can be formed in high populations even in stoichiometric CZTS and CZTSe samples with $Cu/(Zn + Sn) \approx 1$ and $Zn/Sn \approx 1$. Zn rich and Cu, Sn poor conditions are required to decrease their population. In CZTS, $Cu_{Zn} + Sn_{Zn}$ produces a deep donor level, with a localized Sn $5s$ component, and $2Cu_{Zn} + Sn_{Zn}$ causes a significant band gap decrease, which are both detrimental to the solar cell efficiency. However, in CZTSe, the detrimental effects of both clusters are weaker. Based on these results, we provide an explanation for the experimental observation that: (i) kesterite solar cells with the highest efficiencies are fabricated under a Zn rich and Cu, Sn poor conditions, with $Cu/(Zn + Sn) \approx 0.8$ and $Zn/Sn \approx 1.2$; (ii) CZTSSe alloy solar cells have higher efficiencies when the Se composition is high. Experimental identification of the $Cu_{Zn} + Sn_{Zn}$ and $2Cu_{Zn} + Sn_{Zn}$ defect clusters is called for.

[1]T. K. Todorov, K. B. Reuter, and D. B. Mitzi, Adv. Mater. **22**, E156 (2010).

[2]K. Wang, O. Gunawan, T. Todorov, B. Shin, S. J. Chey, N. A. Bojarczuk, D. Mitzi, and S. Guha, Appl. Phys. Lett. **97**, 143508 (2010).

[3]W. Ki and H. W. Hillhouse, Adv. Energy Mater. **1**, 732 (2011).

[4]D. Barkhouse, O. Gunawan, T. Gokmen, T. Todorov, and D. Mitzi, Prog. Photovoltaics **20**, 6 (2012).

[5]S. Bag, O. Gunawan, T. Gokmen, Y. Zhu, T. K. Todorov, and D. B. Mitzi, Energy Environ. Sci. **5**, 7060 (2012).

[6]I. Repins, C. Beall, N. Vora, C. DeHart, D. Kuciauskas, P. Dippo, B. To, J. Mann, W.-C. Hsu, A. Goodrich *et al.*, Sol. Energy Mater. Sol. Cells **101**, 154 (2012).

[7]S. Ahn, S. Jung, J. Gwak, A. Cho, K. Shin, K. Yoon, D. Park, H. Cheong, and J. H. Yun, Appl. Phys. Lett. **97**, 021905 (2010).

[8]S. G. Choi, H. Y. Zhao, C. Persson, C. L. Perkins, A. L. Donohue, B. To, A. G. Norman, J. Li, and I. L. Repins, J. Appl. Phys. **111**, 033506 (2012).

[9]F. Luckert, D. I. Hamilton, M. V. Yakushev, N. S. Beattie, G. Zoppi, M. Moynihan, I. Forbes, A. V. Karotki, A. V. Mudryi, M. Grossberg *et al.*, Appl. Phys. Lett. **99**, 062104 (2011).

[10]X. Fontane, L. Calvo-Barrio, V. Izquierdo-Roca, E. Saucedo, A. Perez-Rodriguez, J. R. Morante, D. M. Berg, P. J. Dale, and S. Siebentritt, Appl. Phys. Lett. **98**, 181905 (2011).

[11]A. Redinger, K. Hoenes, X. Fontane, V. Izquierdo-Roca, E. Saucedo, N. Valle, A. Perez-Rodriguez, and S. Siebentritt, Appl. Phys. Lett. **98**, 101907 (2011).

[12]J. Just, D. Luetzenkirchen-Hecht, R. Frahm, S. Schorr, and T. Unold, Appl. Phys. Lett. **99**, 262105 (2011).

[13]T. Tanaka, T. Sueishi, K. Saito, Q. Guo, M. Nishio, K. M. Yu, and W. Walukiewicz, J. Appl. Phys. **111**, 053522 (2012).

[14]K. Tanaka, Y. Fukui, N. Moritake, and H. Uchiki, Sol. Energy Mater. Sol. Cells **95**, 838 (2011).

[15]B. Shin, O. Gunawan, Y. Zhu, N. A. Bojarczuk, S. J. Chey, and S. Guha, "Thin film solar cell with 8.4% power conversion efficiency using an earth-abundant Cu_2ZnSnS_4 absorber," Prog. Photovoltaics (to be published).

[16]T. Todorov, O. Gunawan, S. J. Chey, T. G. de Monsabert, A. Prabhakar, and D. B. Mitzi, Thin Solid Films **519**, 7378 (2011).

[17]H. Katagiri, K. Jimbo, M. Tahara, H. Araki, and K. Oishi, Mater. Res. Soc. Symp. Proc. **1165**, 1165-M04-01 (2009).

[18]A. Ennaoui, M. Lux-Steiner, A. Weber, D. Abou-Ras, I. Koetschau, H. W. Schock, R. Schurr, A. Hoelzing, S. Jost, R. Hock *et al.*, Thin Solid Films **517**, 2511 (2009).

[19]S.-H. Wei and S. B. Zhang, J. Phys. Chem. Solids **66**, 1994 (2005).

[20]S. Lany and A. Zunger, Phys. Rev. Lett. **100**, 016401 (2008).

[21]S. Chen, X. G. Gong, A. Walsh, and S.-H. Wei, Appl. Phys. Lett. **96**, 021902 (2010).

[22]S. Chen, J.-H. Yang, X. G. Gong, A. Walsh, and S.-H. Wei, Phys. Rev. B **81**, 245204 (2010).

[23]K. Biswas, S. Lany, and A. Zunger, Appl. Phys. Lett. **96**, 201902 (2010).

[24]S. Levcenko, N. Syrbu, E. Arushanov, V. Tezlevan, R. Fernandez-Ruiz, J. Merino, and M. Leon, J. Appl. Phys. **99**, 073513 (2006).

[25]G. Marin, S. Wasim, C. Rincon, G. Perez, P. Bocaranda, I. Molina, R. Guevara, and J. Delgado, J. Appl. Phys. **95**, 8280 (2004).

[26]S.-H. Wei and Y. Yan, *Overcoming Bipolar Doping Difficulty in Wide Gap Semiconductors* (Wiley-VCH Verlag GmbH & Co. KGaA, 2011), pp. 213–239.

[27]S. B. Zhang, S.-H. Wei, A. Zunger, and H. Katayama-Yoshida, Phys. Rev. B **57**, 9642 (1998).

[28]G. Kresse and J. Furthmuller, Phys. Rev. B **54**, 11169 (1996).

[29]S. Lany and A. Zunger, Phys. Rev. B **72**, 035215 (2005).

[30]A. Nagoya, R. Asahi, R. Wahl, and G. Kresse, Phys. Rev. B **81**, 113202 (2010).

[31]S. Chen, X. G. Gong, A. Walsh, and S.-H. Wei, Phys. Rev. B **79**, 165211 (2009).

[32]A. Walsh and G. W. Watson, Phys. Rev. B **70**, 235114 (2004).

[33]S. Chen, X. G. Gong, A. Walsh, and S.-H. Wei, Appl. Phys. Lett. **94**, 041903 (2009).

[34]J. Paier, R. Asahi, A. Nagoya, and G. Kresse, Phys. Rev. B **79**, 115126 (2009).

[35]S. Botti, D. Kammerlander, and M. A. L. Marques, Appl. Phys. Lett. **98**, 241915 (2011).